Needle localization methods in 3D ultrasound data

M. Uherčík[1,2], H. Liebgott[1], J. Kybic[2], C. Cachard[1]

[1]CREATIS-LRMN, Université de Lyon, INSA de Lyon, Université Lyon 1, CNRS, UMR5220, INSERM, U630
INSA - Bâtiment Blaise Pascal, 7, avenue Jean Capelle, 69621 Villeurbanne cedex, F-69621, France
[2]Center for Machine Perception, Department of Cybernetics, Faculty of Electrical Engineering, Czech Technical University
Technická 2, 166 27 Praha 6, Czech Republic, E-mail: uhercik@cmp.felk.cvut.cz

Abstract: Ultrasound imaging has shown to be well adapted for guidance of micro tools, such as biopsy needles or electrodes, in the human body. Indeed it is safe for both patient and physicians, it is cheap and flexible compared to other imaging modalities. The ultrasound imaging offers a real-time acquisition speed but it has to deal with a typical speckle noise and other acoustic artifacts in the image. In clinical practice the tool in ultrasound image is identified by a human expert.

This paper gives an overview of automatic localization methods for needles or electrodes in 3D ultrasound data. We have developed two methods for axis localization: the 1st method is based on Parallel Integral Projection for localization of a straight tool; the 2nd method for axis localization of a curvilinear tool is based on model fitting using a RANSAC algorithm for robust and fast estimation. We present results on phantom data and breast biopsy data.

Key words: 3D ultrasound, biopsy needle, electrode, tool localization, Hough transform, RANSAC.

A. Introduction

Many minimally invasive surgical procedures involve an insertion of a thin tubular instrument into the human body. In a *percutaneous biopsy* (e.g. breast, liver), tissue samples are taken from a region by means of a thin needle [1]. In *prostate brachytherapy*, small radioactive rods are inserted inside the tissue by a hollow shaft [2]. For a *neurological research*, the electrical activity of a specific group of neurons is recorded by a thin electrode [3]. The precise navigation of surgical instruments is vital for reducing the number of failed insertions in the tissue.

A *stereotactic frame* for instrument guidance was first introduced by [4] on small animals. The frame is fixed with respect to external anatomical landmarks. To avoid the limitations of the frame and the patient discomfort, *frameless techniques* were proposed, e.g. the spatial localization of tool using a magnetic sensor [5], and optical tracking with two calibrated cameras [6]. Nowadays, the stereotaxy is often combined with *medical imaging techniques* (e.g. MRI, CT, or ultrasound imaging) [7] which permit localization accuracy of the order of a tenth of a millimeter. Physicians can view anatomical information of the human body together with surgical instruments during the intervention.

In clinical practice, visual localization is done by a human expert. In common 2D ultrasound imaging; the physician must be trained to *maintain the observation plane* incident with the tool. This can be partially solved by fixing the needle to the probe [8]. Using the 3D ultrasound, the full volume of interest is observed and the guidance task becomes easier, but requires more processing time.

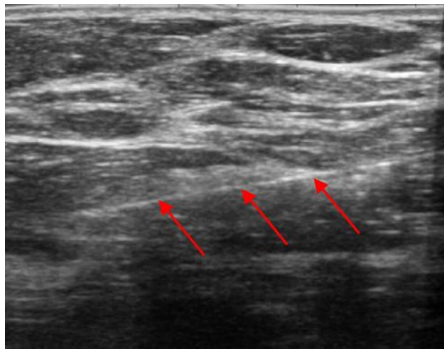

Figure 1: an example of 2D ultrasound image containing a needle (marked by arrows) in the breast tissue.

The ultrasound imaging of micro-surgical tools offers a *real-time acquisition speed*, the cost is relatively modest and it does not produce any ionizing radiation. It is affected by a *strong speckle noise*, but the tool of higher stiffness usually appears as high intensity in the ultrasound image. Some types of tissue (e.g. fat, bones) have similar high-intensity appearance like the tool which makes the segmentation difficult (Figure 1). The resolution of modern systems is approximately 1 mm, depending on the central frequency.

B. Localization methods in ultrasound

A variety of algorithms for object localization in ultrasound data have been proposed. The position of an axis of an object such as an electrode can be determined in a 2D image using the *principal component analysis* [9]. The experiments with a breast biopsy needle of 2.1 mm in diameter show that the intercept and the needle tip can be determined by the algorithm with accuracy of 1 mm for a depth of insertion greater than 15 mm.

To find the straight tool in an ultrasound image, the *Hough Transform (HT)* can be used for the line detection. The projection of tool is minimized to a single point when the projection is performed along the tool axis. Ding [10] proposed to use *2D projections of 3D* ultrasound volume for faster detection of needle. Wei [11] uses this method for 3D for guidance of robot-aided prostate brachytherapy. Testing showed that the algorithm can find 3D needle orientation within 0.54° for a chicken tissue phantom, and 0.58° for agar phantoms, over a ±15° insertion orientation. Qui [12] introduced a quick *randomized 3D Hough Transform*, but the experiments were done only in water tank yet.

Okazawa [13] generalized the HT for detection of *curved needles* in 2D ultrasound images at real-time speed. They tested the method on ultrasound images of a phantom and on photographic images. Salcudean [14] developed a robotic needle guide for prostate brachytherapy based on this method and he reported 0.06 mm translational repeatability.

A modified Radon Transform was proposed by Novotny [15] which is similar to 3D HT. They divided the volume to smaller regions and detected the axis locally using a fast method on a *graphics processing unit*. They demonstrated a real-time tracking of tubular instruments of diameter 5 mm in a cardiac sequence with accuracy 0.2 mm.

C. Proposed methods

The following *assumptions* about the tool appearance are made: (i) the intensity of tool voxels is higher than the surrounding voxels because of different acoustic impedance, and (ii) the tool appears as a cylindrical object with a possibly bended axis and a length much greater than a diameter.

Proposed localization algorithms works in two steps: (1) *Axis localization* – the approximate position and orientation. We present two methods for axis localization: Parallel Integral Projection (PIP) transform (Section C.1), model fitting by a randomized algorithm (Section C.2). (2) *Tip localization* – once the axis is known, the endpoint of the tool is localized, the values of all voxels along the axis are considered to identify the tip of the tool [16]. A thresholding is done and a morphological closure is applied to skip small breaks in the tool caused by speckles in the ultrasound image.

C.1. Axis localization by PIP transform

We propose to maximize the PIP transform to localize a straight cylindrical object in 3D images [17]. The PIP is formalized as a transform that maps an image function $I: \mathbb{R}^3 \to \mathbb{R}$ representing volume data to a function $P_I: \mathbb{R}^4 \to \mathbb{R}$ describing its projections as a function of the 2D displacement (u, v) and the projection direction determined by two angles (α, β). More formally, the PIP transformation of $I(x)$ is defined by an integral along a line passing through the point $Q = [u, v]$ with direction w given by angles (α, β):

$$P_I(u, v, \alpha, \beta) = \int I(R(\alpha, \beta) \cdot (u, v, \tau)^T)\, d\tau, \qquad (1)$$

where $R(\alpha, \beta)$ is the rotation matrix representing a rotation around the x-axis by angle α, and around the y-axis by angle β. The PIP transform is similar to the HT [18] but it uses only 2 accumulators representing the angle. The PIP transform is also a form of the generalized Radon transform used in CT [19].

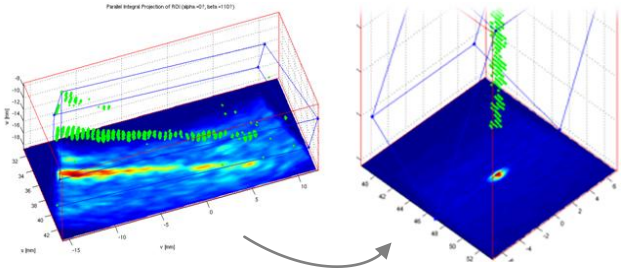

Figure 2: Two examples of PIP Transform – there is a group of thresholded voxels in green and a projection plane in each image. Left picture contains a tool in an arbitrary position; right picture shows an ideal orientation of tool perpendicular to the projection plane.

The location of the PIP maximum (Figure 2)

$$(u_{max}, v_{max}, \alpha_{max}, \beta_{max}) = \arg\max P_I(u, v, \alpha, \beta), \qquad (2)$$

approaches the axis with a parametric equation:

$$a(t) = R(\alpha_{max}, \beta_{max}) \cdot (u_{max}, v_{max}, t)^T;\ \forall t \in \mathbb{R}. \qquad (3)$$

The maximization of $P_I(u, v, \alpha, \beta)$ can be done by a slow exhaustive evaluation of the whole angle space (α, β). A proper discretization of the angle space must be set [17]. Efficient techniques for finding the maximum have been proposed: (a) hierarchical mesh-grid search [17], (b) multiple resolutions down-sampling [20], (c) and early stopping of the optimization [20]. The combination of all three techniques can lead to a rapid improvement of the speed, but the robustness of the method is not so good in case of presence of other high-intensity appearance structures.

C.2. Model fitting of axis with RANSAC

The estimator *RANSAC* (RANdom SAmple Consensus) was introduced by [21]. We propose to use it for a curvilinear tool axis localization in 3D ultrasound data [16] which is fast and robust to presence of noise and other high-appearance structures. Given an input data, RANSAC iteratively tries to fit a model to it using a cost function. Such model is chosen which maximizes the cost for the input data.

Using Assumption (i), the input volume $X = \{x \in R^3\}$ is *thresholded* with a pre-computed threshold T_I; so later we work with voxels $X_t = \{x \mid I(x) > T_I\}$. The idea behind it is to reduce the amount of data and computational time.

The *model* of axis that we want to find is a polynomial curve $a(H, t)$ of order D represented by

matrix H of size 3x3:

$$a(H;t) = H \cdot (1, t, t^2 \dots t^{D-1}); t \in \mathbb{R}. \quad (4)$$

The parameters H can be computed from D control points in the space. The straight line or polynomial curve of higher order can be used depending on the expected deformation of tool.

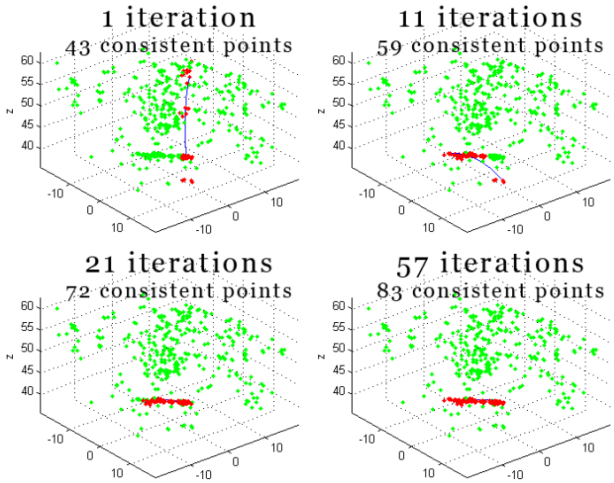

Figure 3: Tool models found by RANSAC in subsequent iterations on a thresholded dataset of 399 voxels. The red points are inliers (consistent points) and the green points are outliers. The estimated curve is marked by blue colour. After 57 iterations the solution with 83 inliers has been found.

Two models are presented in [16]: (i) *AxShp* – computing only the distance of thresholded voxels to the axis, (ii) *IntDstr* – evaluating the intensity of voxels close to the axis and comparing them to a typical intensity profile. The second model is using a pre-computed 2D distribution $p(I,r)$ of a voxel intensity I and a distance $r = dist(l,x)$ from the axis.

The axis is estimated by the RANSAC procedure which uses a *error function* $E(x;H)$ which represents the penalty associated to voxel x with respect to current model H. If the error function $E(x;H)$ is less than a threshold Δ, then the voxels is called an *inlier*. The RANSAC iteratively tries models defined by D random sample of points, and finds the best model which is associated by maximal the number inliers $|X_{inl}|$ *(Figure 3)*.

The accurate solution is obtained by a *local optimization* using the simplex algorithm [22] of the curve parameters H on the set on inliers X_{inl} because it does not need any derivative information.

D. Results

The proposed methods have been tested on simulated data, on real data of phantom and breast biopsy. Two measures are used to assess the accuracy of the proposed method [16]. The *tip* localization *accuracy* ε_{tip} measures the Euclidean distance to ground-truth tip. The *axis* localization *accuracy* ε_{axis} measures the maximal orthogonal distance of localized axis and ground-truth axis.

The data mimicking a breast tissue was created using a software package Field II [23]. The tool with appropriate acoustic parameters was added in the radio-frequency signal domain. Afterwards, 3D envelope images were calculated. An example of such volume is in Figure 4. The tests on simulated data show the behaviour of the localization under different conditions. The results of the simulation study can be found in [24].

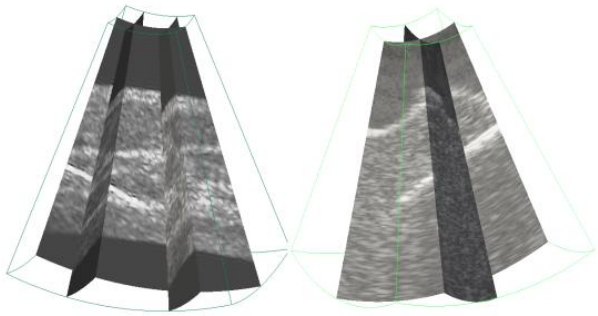

Figure 4: A 3D visualization of our phantoms: on left picture, a simulated data with inhomogeneous background; on right side, a PVA Cryogel phantom with a tungsten electrode (the *volume* size is 53x71x164 voxels).

To mimic biological tissue with a highly reflecting inclusion, a polyvinyl alcohol (PVA) Cryogel phantom [25] was created. Inside the phantom there was a thin tungsten electrode of 150 μm in diameter and length 20 mm. The phantom was scanned with a ultrasound scanner Voluson 530D with a 3D probe operating at central frequency 7.5 MHz. The axial resolution was 0.4 mm and the lateral resolution was approximately 1 mm. The results can be found in the Table 1 and 2:

Table 1: Results of axis localization.

Method	ε_{axis} *[mm]*	*Time [sec]*
PIP transf. [17]	0.15 – 0.2	61 – 62
MR PIP [20]	1.4 – 3.2	5.5 – 7.3
RANSAC [16]	0.3 – 0.6	0.6 – 1

Table 2: Results of tip localization.

Method	ε_{tip} *[mm]*	*Time* [sec]
Tip localization	0.79	0.5

The proposed methods were also tested on real ultrasound datasets of breast biopsy. The datasets were acquired by the 3D scanner GE Voluson E8 with the probe operating at the central frequency of 12 MHz. Inside the tissue, there was a 19-gauge needle made of stainless steel. The localization algorithm was successful using the RANSAC method. The axis accuracy was 0.36 ± 0.19 mm and the elapsed time was 0.62 second. The tip of the needle was located outside of the scanned volume area.

E. Conclusion

We presented a survey of tool localization methods in ultrasound images which were based mostly on HT. We have developed two localization methods working on the 3D ultrasound images capable to localize the micro-tools of very small diameter (up to 150 μm). Unlike the HT-based methods, the model fitting with RANSAC shows as fast and robust method also on real data of breast biopsy. This localization algorithm was able to detect the biopsy needle in a real tissue of breast. More robust model could be developed by taking into account more a priori information about the shape and appearance of the tool in ultrasound images, e.g. 1-dimensionality of the tool.

F. Acknowledgements

We would like to thank to Daniel Buckton and Christian Perrey from GE Medical Systems for providing us the 3D ultrasound data of breast biopsy.

The author M. Uherčík was supported by an EC project MEST-CT-2005-021024 WARTHE (Wide Applications Research Training in Health Engineering). The author J. Kybic was supported by Czech Ministry of Education project MSM6840770012.

G. References

[1] A. Abati and A. Simsir, "Breast fine needle aspiration biopsy: prevailing recommendations and contemporary practices." 4, December 2005, Clinics in laboratory medicine, Vol. 25, pp. 631-654.

[2] Merrick, G.S., et al. "Monotherapeutic brachytherapy for clinically organ-confined prostate cancer." 4, August 2005, West Virginia Medical Journal, Vol. 101, pp. 168-171.

[3] Alterman, R.L., et al. "Microelectrode recording during posteroventral pallidotomy: Impact on target selection and complications." 2, February 1999, Neurosurgery, Vol. 44, pp. 315-321.

[4] Horsley, V. and Clarke, R.H. "The structure and functions of the cerebellum examined by a new method." 1908, Brain, Vol. 31, pp. 45-124.

[5] Glossop, N.D., et al. "Needle tracking using the aurora magnetic position sensor." Santa Fe, USA, 2002. CAOS 2002.

[6] Krueger, S. , et al. "Evaluation of Computer-assisted Image Enhancement in Minimal Invasive Endoscopic Surgery." 2004, Methods of Information in Medicine, Vol. 43 , pp. 362-366.

[7] Peters, T.M. "Image-guidance for surgical procedures." 14, 2006, Physics in Medicine and Biology, Vol. 51.

[8] Wedel, Pruter. "Needle guide for ultrasound transducers." *Patent no. 5,052,396* USA, 1991.

[9] Draper, K. J. , et al. "An algorithm for automatic needle localization in ultrasound-guided breast biopsies." 2000, Medical Physics, Vol. 27, pp. 1971-1979.

[10] Ding, M. and Fenster, A. "A real-time biopsy needle segmentation technique using Hough Transform." Aug 2003, Medical Physics, Vol. 30, pp. 2222-2233.

[11] Wei, Z. , et al. "Oblique needle segmentation and tracking for 3D TRUS guided prostate brachytherapy." 9, Sep 2005, Medical Physics, Vol. 32, pp. 2928-2941.

[12] Qiu, W., Ding, M., Yuchi, M. "Needle Segmentation Using 3D Quick Randomized Hough Transform." 2008. Proceedings of ICINIS. pp. 449-452. 978-0-7695-3391-9.

[13] Okazawa, S.H., et al. "Methods for segmenting curved needles in ultrasound images." 3, 06 2006, Medical image analysis , Vol. 10, pp. 330-342.

[14] Salcudean, S.E. , et al. "A robotic needle guide for prostate brachytherapy." 2008. Proceedings of ICRA. pp. 2975-2981.

[15] Novotny, P.M., et al. "GPU Based Real-time Instrument Tracking with Three Dimensional Ultrasound." 2007, Medical image analysis, Vol. 11, pp. 458-464.

[16] Barva, M. "Localization of Surgical Instruments in 3D Ultrasound Images." Center for Machine Perception, K13133 FEE Czech Technical University. Prague, Czech Republic, 2007. PhD Thesis.

[17] Barva, M., et al. "Parallel Integral Projection Transform for Straight Electrode Localization in 3-D Ultrasound Images." 7, July 2008, IEEE Transactions on Ultrasonics, Ferroelectrics, and Frequency Control, Vol. 55, pp. 1559-1569.

[18] Duda, R.O. and Hart, P.E. "Use of the Hough Transformation to Detect Lines and Curves in Pictures." Comm. ACM. 15, 1972, pp. 11-15.

[19] Natterer, F. "The Mathematics of Computerized Tomography." SIAM: Society for Industrial and Applied Mathematics, 2001. ISBN 0898714931.

[20] Uherčík, M., et al. "Multi-resolution Parallel Integral Projection for Fast Localization of a Straight Electrode in 3D Ultrasound Images." Proceedings of the ISBI 2008. pp. 33-36.

[21] Fischler, M.A. and Bolles, R.C. "Random sample consensus: A paradigm for model fitting ..." Communications of ACM. 24, June 1981, Vol. 6, pp. 381-395.

[22] Nelder and Mead. "A simplex method for function minimization." The Computer Journal. 7, 1965, pp. 308-313.

[23] Jensen. "A program simulating ultrasound systems." Medical and Biological Engineering and Computing. 34, 1996, pp. 351-353.

[24] Barva, M., et al. "Comparison of Methods for Tool Localization in Biological Tissue from 3D Ultrasound Data." Proceedings of the IEEE Ultrasonics Symposium 2006. pp. 1983-1986. ISBN 1-4244-0202-6.

[25] Chu and Rutt. "Polyvinyl alcohol: An ideal phantom material for MR studies of arterial flow and elasticity." Magnetic Resonance in Medicine. 37, 1997, Vol. 2, pp. 314-319.